

## CATALOGUE OF ORBITS OF NEARBY STARS: PRELIMINARY RESULTS

A. A. MÜLLÄRI<sup>1</sup>, T. B. MÜLLÄRI<sup>1</sup>, V. V. ORLOV<sup>2</sup>, and A. V. PETROVA<sup>2</sup>

<sup>1</sup> *Mathematical faculty, Petrozavodsk State University, Lenin prospect 33,  
Petrozavodsk 185640, Karelia, Russia*

<sup>2</sup> *Astronomical Institute, St. Petersburg State University, Bibliotechnaya pl. 2,  
St. Petersburg 198904, Peterhof, Russia*

(Received May 21, 1996)

A catalogue of the orbits of 1946 nearby stars from the solar neighbourhood within 25 pc has been compiled. The typical examples of the orbits in projection to the meridional plane are given. The overwhelming majority of orbits are box-like. Also box orbits with folds, banana and tube orbits are found. The distributions of eccentricities and relative semi-heights of the orbits are constructed. The correlations between the orbital elements and absolute magnitudes of the residual space velocities are given. The types of stellar orbits for different galactic subsystems are discussed.

**KEY WORDS** Nearby stars: galactic orbits

Three characteristics of the galactic structure and kinematics have an essential cosmogonic interest, as these have to reflect a process of formation and evolution of different galactic subsystems: thin and thick discs, halo, and bulge. One can find information on the structure and kinematics of the Galaxy using the data on the coordinates and space velocities of various galactic objects: stars, stellar clusters, gaseous clouds, etc.

The *Catalogue of Nearby Stars* (Gliese and Jahreiss, 1991, unpublished) from the solar neighbourhood within 25 pc is the most complete sample of the stars. This catalogue contains the heliocentric coordinates ( $\alpha, \delta, \pi$ ) and space velocities ( $U, V, W$ ) for 1946 stars. As the stars considered occupy a very small portion of the galactic volume, one can not judge the whole galactic structure by these stars. At the same time, the space velocities of the stars are distributed within a rather wide interval and may give useful information on the kinematics of the Galaxy and its subsystems.

The galactic kinematics is described by not only the distribution of the space velocities observed  $f(U, V, W)$ , but also by that of the orbital elements for the stars under consideration. In order to define the orbital type and elements via the data of observations one needs to have a dynamical galactic model. A number

of such models is known from the literature (see, e.g. Allen and Martos, 1986; Binney and Tremaine, 1987; Kutuzov and Ossipkov, 1989; Allen and Santillan, 1993, and references therein). All available dynamical galactic models have rotational symmetry and are stationary, i.e. the potential does not depend on time. Both these assumptions do not reflect the actual situation as a whole, because the Galaxy has a spiral structure and, possibly, a central bar. The structure of subsystems does vary with time; e.g. heating of the disc takes place due to scattering of the stars by the giant molecular clouds and other objects of the disc. The stationarity of the model has been assumed and the irregular forces have been neglected because we are interested in the stellar orbits as kinematical tracers, and the actual motions of the stars in the Galaxy.

We have chosen the model of Kutuzov and Ossipkov (1989) for calculations. The model has two components: core + bulge and disc + halo. The galactic potential in this model is as follows:

$$\Phi(R, z) = \Phi_0[a\phi_a(\xi) + b(\phi_b(r))], \quad a + b = 1, \quad (1)$$

where  $\Phi_0 = \Phi(0, 0)$  is the potential in the galactic centre,  $a$  and  $b$  are the weights of the components, and  $\phi_a$  and  $\phi_b$  are their dimensionless potentials:

$$\phi_a(\xi) = \alpha[\beta + (1 + \kappa\xi^2)^{1/2}]^{-1}, \quad (2)$$

where  $\beta = \alpha - 1$ ,  $\xi^2 = r^2 + 2(1 - \epsilon)[(\epsilon^2 + \zeta^2)^{1/2} - \epsilon]$ ,  $r = (\rho^2 + \zeta^2)^{1/2}$  and

$$\phi_b(r) = (1 + \lambda r)^{-1}, \quad (3)$$

where  $\rho = R/r_0$ ,  $\zeta = z/r_0$ ,  $R$ ,  $z$  are cylindrical coordinates ( $R$  is the distance from the galactic rotation axis,  $z$  is the distance from the galactic plane); and  $r_0$  is the scale length. The model has two scale parameters ( $r_0$ ,  $\Phi_0$ ) and five structural parameters ( $\alpha$ ,  $\kappa$ ,  $\epsilon$ ,  $\lambda$ ,  $a$ ). The following values of parameters taken from Kutuzov and Ossipkov (1989) are used:

$$(r_0, \Phi_0) = (2.54 \text{ kpc}, 3.81 \times 10^5 \text{ km}^2 \text{ s}^{-2});$$

$$(\alpha, \kappa, \epsilon, \lambda, a) = (4.17, 0.69, 0.11, 6.60, 0.37).$$

The equations of motion for each of the 1946 stars were integrated during  $5 \times 10^9$  years. The Runge–Kutta–Fehlberg 5(6) order integrator was used with an automatic choice of the step. Checking of the calculations was carried out using the energy conservation. The relative errors of this integral to the end of computations were  $10^{-6}$ – $10^{-8}$ .

The minimum  $R_p$  and maximum  $R_a$  distances from the galactic centre were estimated, as well as the maximum deviation  $z_m$  from the galactic plane. Using these values, the orbital elements were found — eccentricity:

$$e = \frac{R_a - R_p}{R_a + R_p}, \quad (4)$$

**Table 1.** Statistical parameters (expectations  $\bar{X}$ , rms deviations  $\sigma_X$ , medians  $X_{1/2}$ , and quartiles  $X_{1/4}$ ,  $X_{3/4}$ ) of the distributions of orbital elements and absolute magnitudes of the residual velocities  $v$

<i>Name</i>	$\bar{X}$	$\sigma_X$	$X_{1/2}$	$X_{1/4}$	$X_{3/4}$
<i>e</i>	0.147	0.120	0.112	0.069	0.191
<i>h</i>	0.019	0.035	0.010	0.004	0.021
<i>v</i>	52.2	41.4	42.5	26.9	64.5

and relative semi-height:

$$h = \frac{z_m}{R_a + R_p}. \quad (5)$$

The distributions of these elements  $f(e)$  and  $f(h)$  are shown in Figures 1 and 2. The maxima of the distributions are in a region of small values, at  $e = 0.07$  and  $h = 0.003$ . Therefore the intervals  $e \in [0, 0.3]$  and  $h \in [0, 0.1]$  are shown in the figures only. The distributions outside these intervals are monotonous decreasing functions at larger  $e$  and  $h$ . We do not show the larger intervals in order to reach a better resolution within the more populated regions. The small secondary maxima are seen in the histograms, but these are insignificant, i.e. the clear separation into subsystems is not observed in the solar neighbourhood.

The statistical parameters of the distributions are given in Table 1, as well as those of the residual stellar velocities  $v$  (their modules). The expectations, rms deviations, medians, and quartiles are presented. The distributions are strongly asymmetric: most orbits have small eccentricities and are strongly flattened to the galactic plane. The stars of galactic disc have such orbits. As the same time, there is a rather small number of orbits with very small eccentricities which are typical for a young disc population. Thus the young stars are not numerous in the nearest solar neighbourhood. The growth of orbital eccentricities, as well as the thickening of the orbits may be connected with scattering of the disc stars on the giant molecular clouds, because the velocity dispersion of the disc stars increases due to this effect.

Let us consider the dependences between values  $e$ ,  $h$  and the absolute magnitude of the residual velocity  $v$ . These dependences are shown in Figures 3–5. Figures 3–5*a* show the whole diagrams, while Figures 3–5*b* present cut-down diagrams in the vicinity of zero. Figures 6*a* and *b* show the three-dimensional diagrams which give the dependence between these three parameters. The cut-down diagrams give more detailed information on the behaviour of these parameters for the most populated sample of the galactic disc. Also the coefficients of correlation between these parameters were calculated:

$$r(v, e) = 0.917 \pm 0.004, \quad r(h, e) = 0.507 \pm 0.017, \quad r(v, h) = 0.559 \pm 0.016.$$

As expected, a strong positive correlation is observed. An especially clear dependence between  $e$  and  $v$  exists (Figure 3). In Figure 4 (dependence between  $h$  and  $v$ ), a region of avoidance along the axis  $h$  is found. The origin of this region is obvious, because in order to reach a significant  $z_m$  the star has to have a large velocity  $v$ .

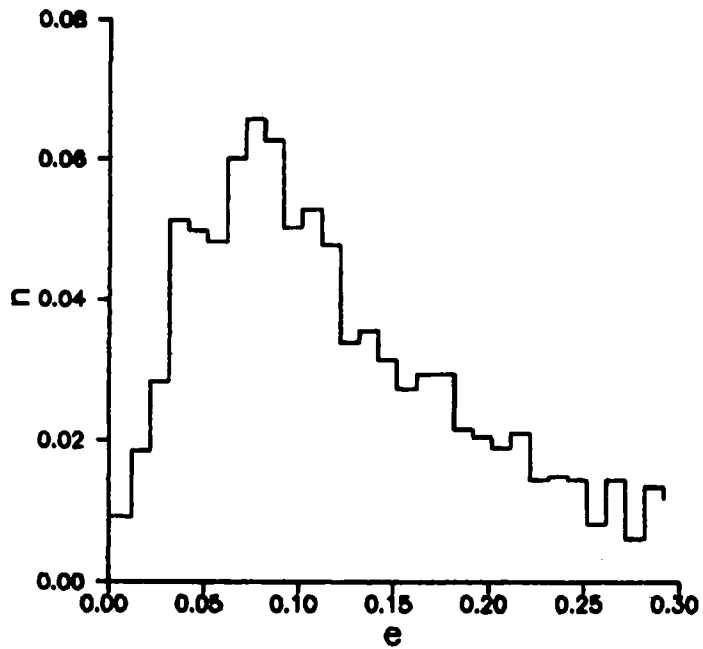


Figure 1 Distribution of orbital eccentricities.

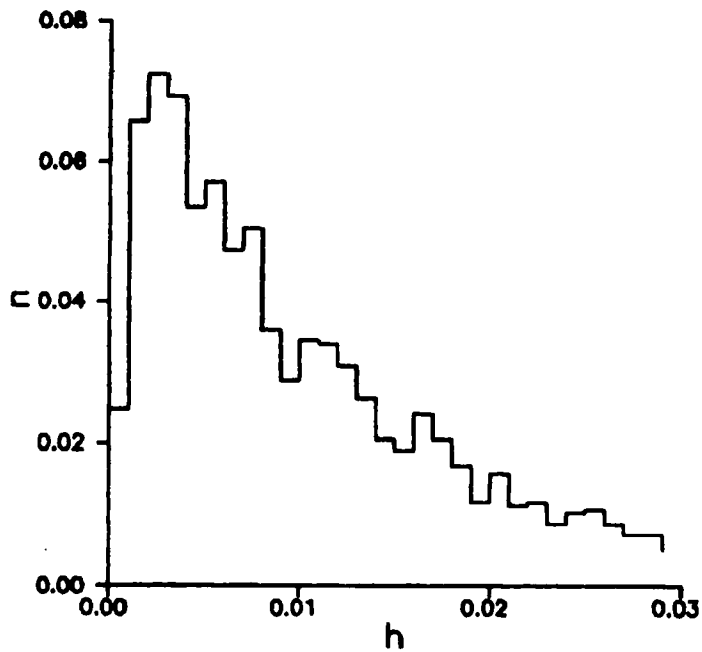


Figure 2 Distribution of relative semi-heights of orbits.

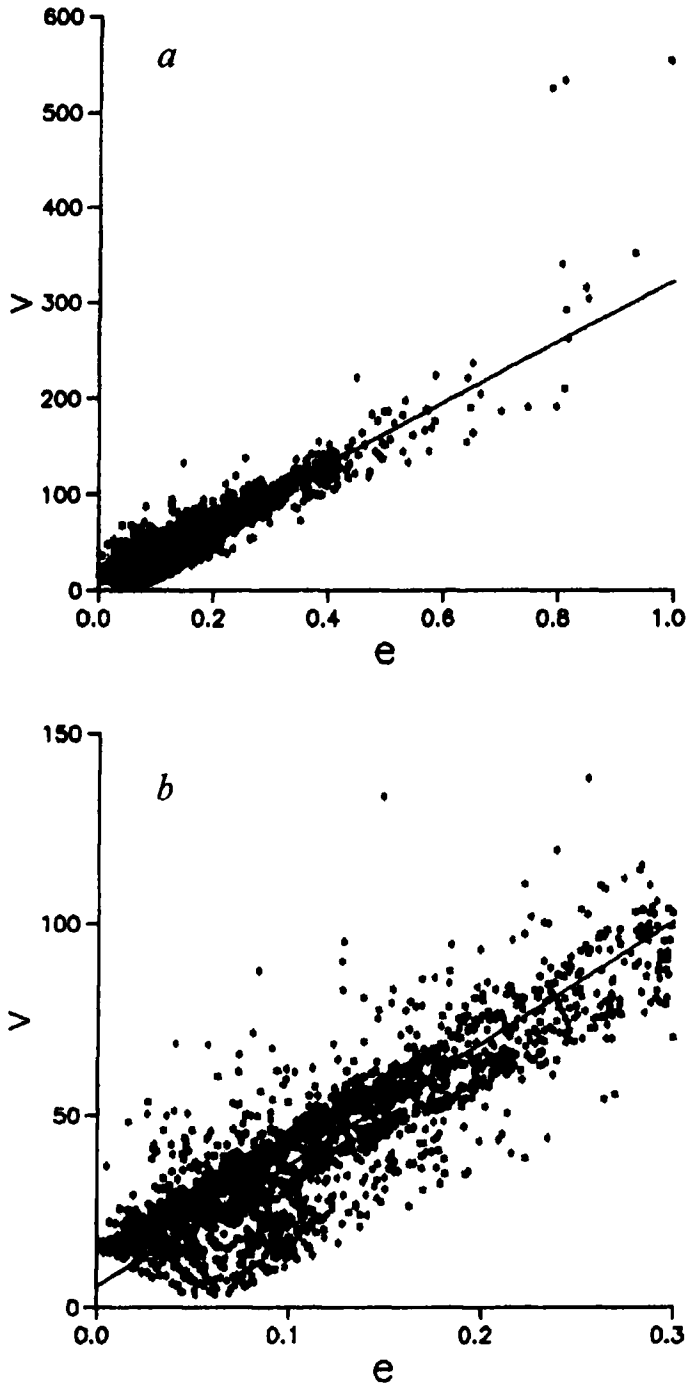


Figure 3 Dependence between eccentricity  $e$  and absolute magnitude of residual velocity  $v$ : *a*, whole diagram; *b*, cut-down diagram. The straight line is the least-squares fit.

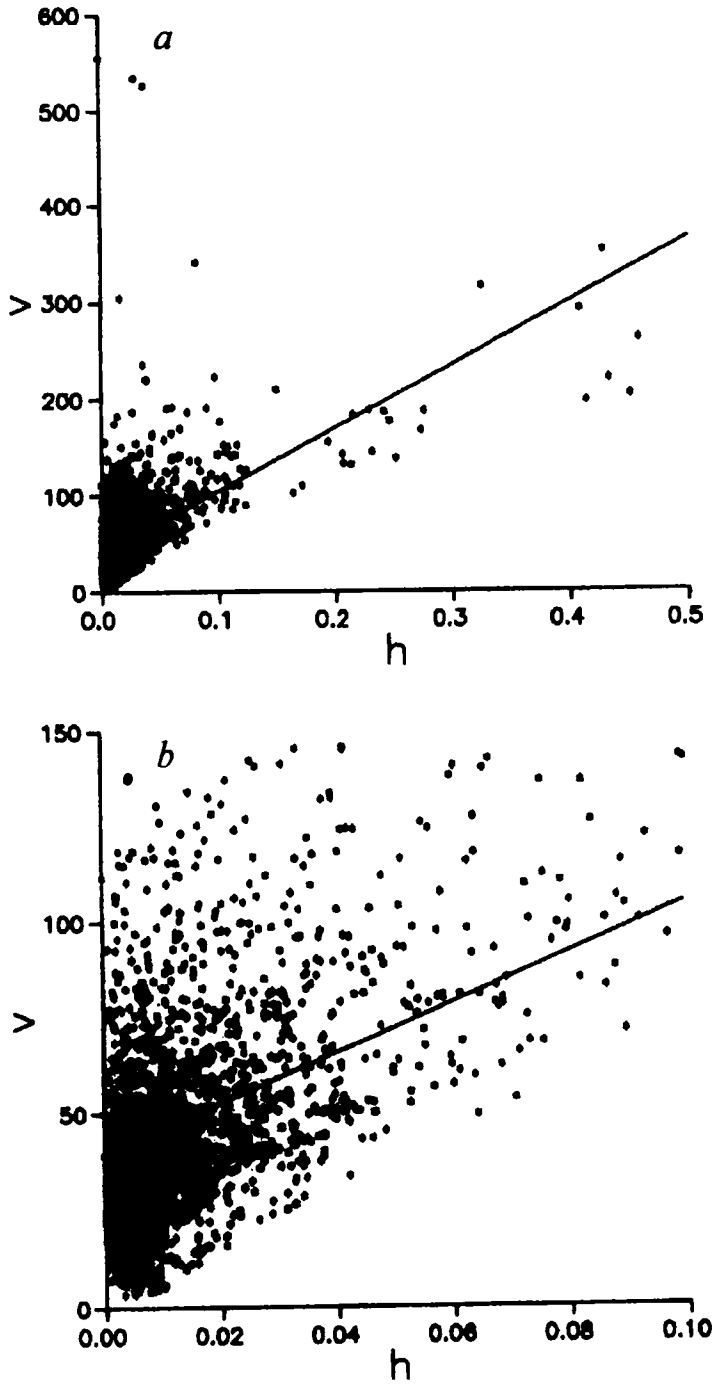


Figure 4 Dependence between relative semi-height  $h$  and absolute magnitude of residual velocity  $v$ : *a*, whole diagram; *b*, cut-down diagram. The straight line is the least-squares fit.

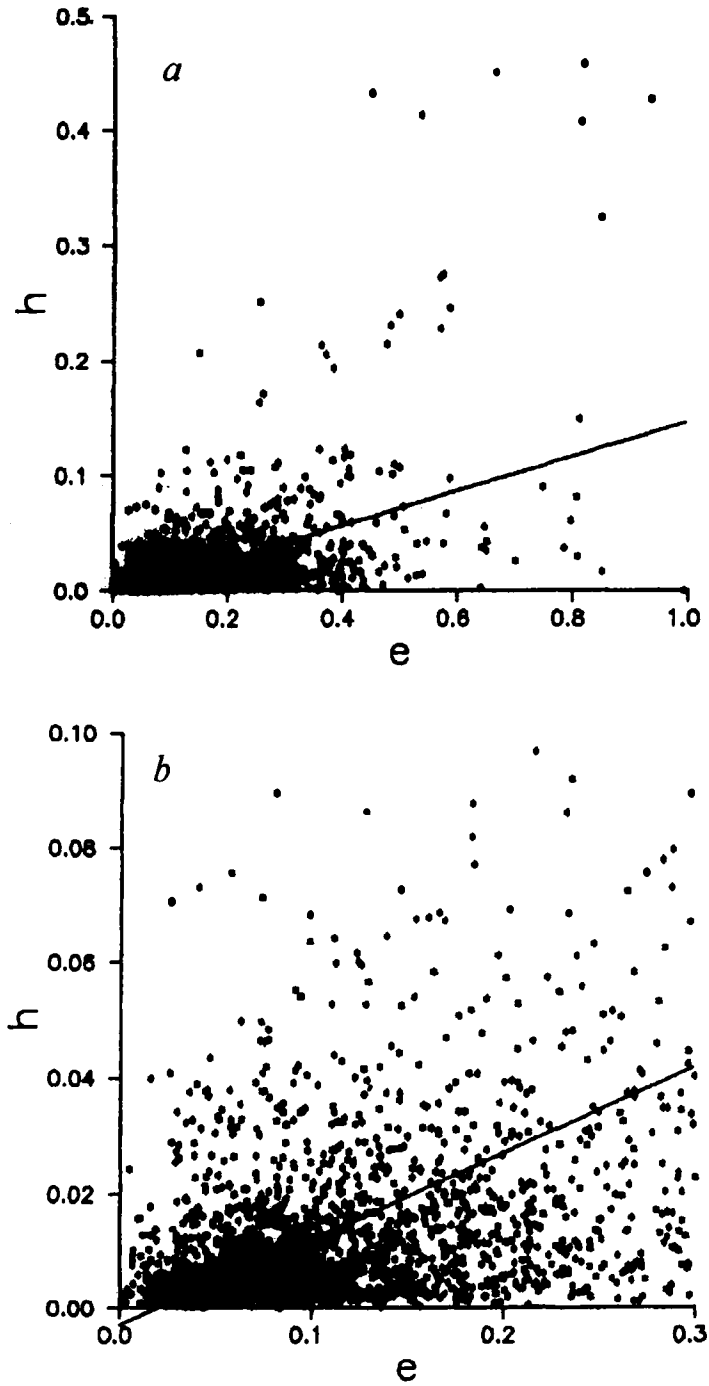
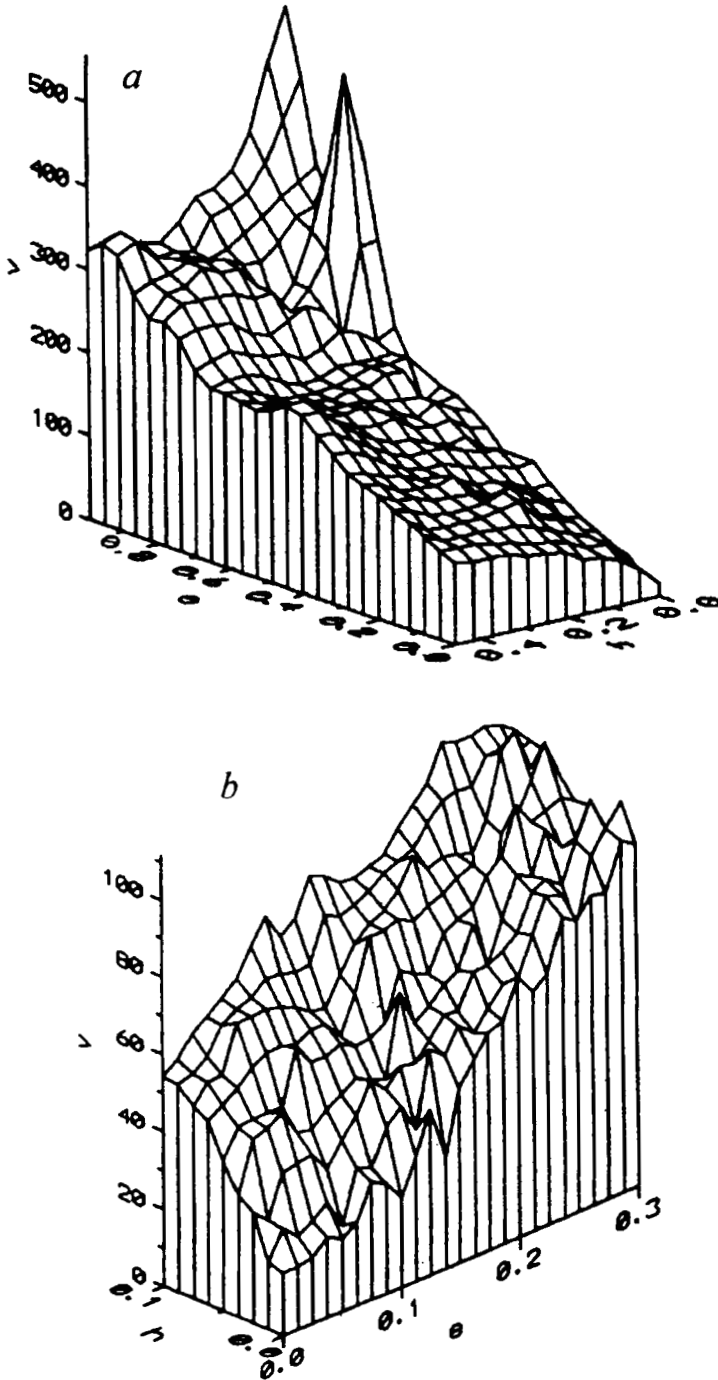


Figure 5 Dependence between eccentricity  $e$  and relative semi-height  $h$ : *a*, whole diagram; *b*, cut-down diagram. The straight line is the least-squares fit.



**Figure 6** Three-dimensional dependence between  $e$ ,  $h$  and  $v$ : *a*, whole diagram; *b*, cut-down diagram near zero.



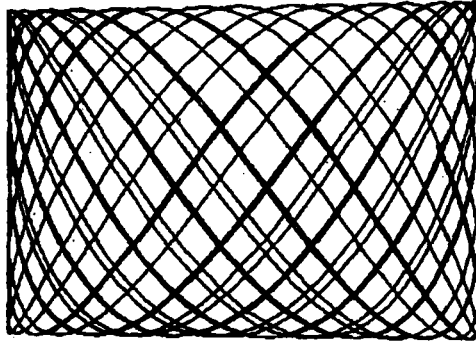


Figure 7 Typical box-like orbit without folds in the meridional plane (star G1 5).

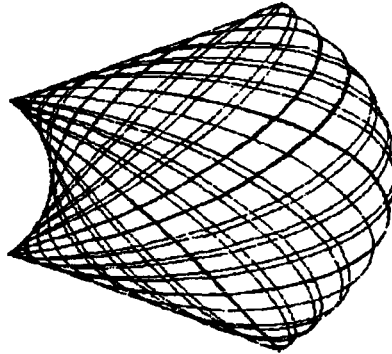
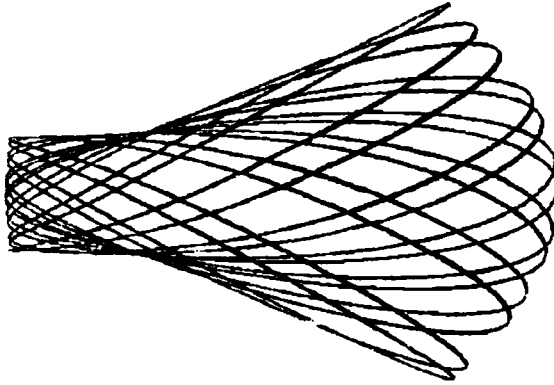


Figure 8 Box-like orbit with curved walls of the box (star GJ 2005).

The border of this region is similar to a parabola. The points of the dependence between  $h$  and  $e$  (Figure 5) are concentrated on the axis  $e$ , i.e. the velocity dispersion along the radius is large than that along the  $z$ -coordinate.

The trajectories of the stars in projection to the meridional (comoving) plane were drawn. A few trajectories of various types are shown in Figures 7–15. A preliminary examination of the pictures has shown that orbits of the following types are observed: (1) box-like orbits (with and without folds) (Figures 7–10); (2) banana orbits (with and without folds) (Figures 11 and 12); (3) tube orbits (Figure 13); (4) possible ergodic orbit (Figure 14) (its origin may be connected with accumulated errors of calculations). Some of the orbits are close to periodic ones (see, e.g. Figure 15). The overwhelming majority of the stars in the sample under consideration have simple box-like orbits without folds (as in Figure 7). One star (G1 473 A) has a hyperbolic orbit and leaves the Galaxy.

Possibly, orbits of different types are habitual in different galactic subsystems. For example, stars in a thin disc have box orbits, while stars in a thick disc and halo may have at the same time box orbits with folds, tube and banana orbits.



**Figure 9** Box orbit with two folds (star GJ 1062).

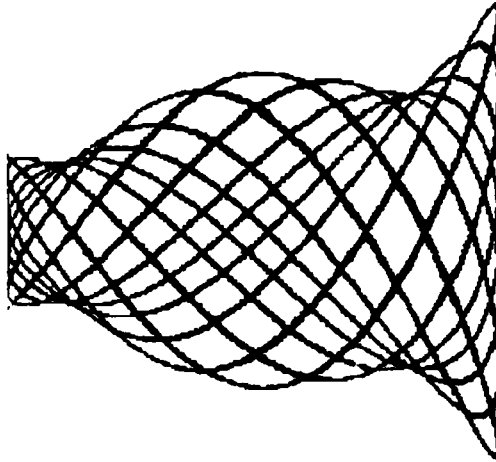


**Figure 10** Box orbit with four folds (star GJ 451).

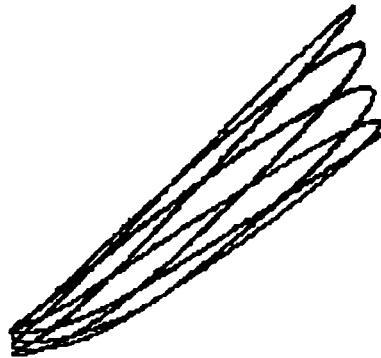


**Figure 11** Banana orbit without folds (star GJ 1104).

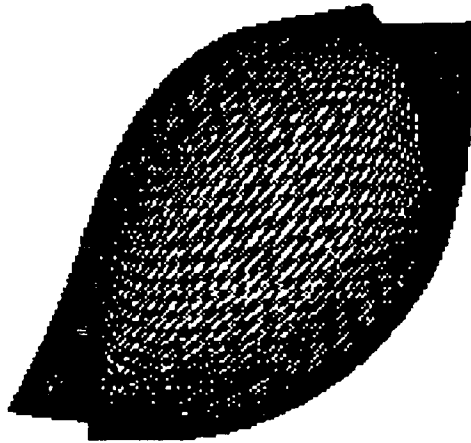


**Figure 12** Banana orbit with two folds (star Wo 9281).

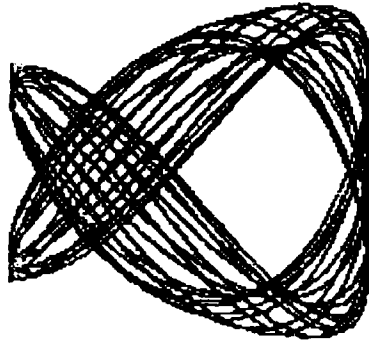


**Figure 13** Tube orbit (star GJ 1252).

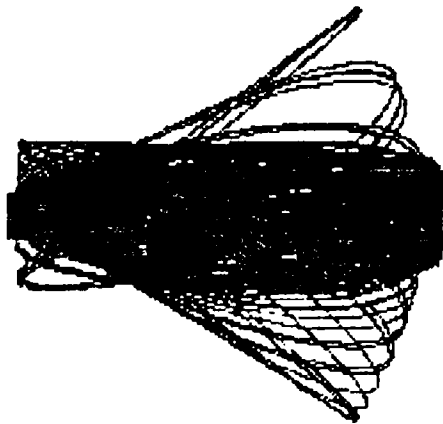


**Figure 14** Ergodic orbit (star Gl 699.1).

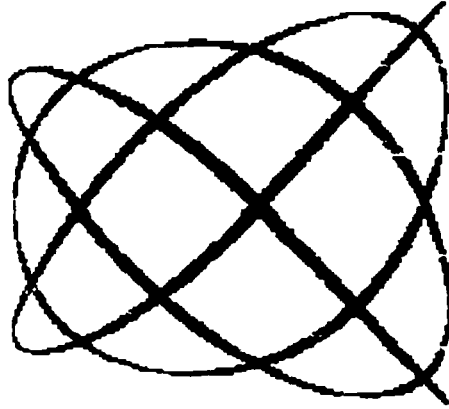


Figure 15 Orbit close to the periodic one (star Gl 118).

One can formulate the following conclusions from the above results.

- (1) The overwhelming majority of stars in the solar neighbourhood have box orbits, these are from the disc of the Galaxy.
- (2) The distributions of orbital eccentricities  $e$  and relative semi-heights  $h$  are nonmonotonous and strongly asymmetric: orbits with small, but non-zero values of  $e$  and  $h$  dominate.
- (3) The secondary maxima on the distributions of  $e$  and  $h$  are statistically insignificant, i.e. clear subsystems are absent in the solar neighbourhood.

### References

- Allen, C. and Martos, M. (1986) *Rev. Mex. Astron. Astrofis.* **13**, 137.  
 Allen, C. and Santillan, A. (1993) *Rev. Mex. Astron. Astrofis.* **25**, 39.  
 Binney, J. and Tremaine, S. (1987) *Galactic Dynamics*, Princeton University Press.  
 Gliese, W. and Jahreiss, H. (1991) *Catalogue of Nearby Stars*, unpublished.  
 Kutuzov, S. A. and Ossipkov, L. P. (1989) *Astron. Zh.* **66**, 965.